

Quantum chaos and macroscopic realism as no-signaling in time

Manish Ramchander*

Institute of Mathematical Sciences, Taramani, Chennai 600113, India

Arul Lakshminarayan†

Department of Physics, Indian Institute of Technology Madras, Chennai 600036, India

Abstract

Macroscopic realism is a set of assumptions about how we experience the world at a classical level. While the Leggett-Garg inequalities are temporal correlations that are violated by quantum systems not obeying such macrorealism, the no-signaling in time condition is also a necessary condition. This compares measurement outcomes with and without prior measurements. As dynamics and correlations play a central role in these measures, this paper explores the effects of regular versus chaotic dynamics on the violations of macroscopic realism. We observe a close connection between a 3 point out-of-time-order correlator and the conditional probabilities of measurement, and we find unmistakable imprints of chaos on the violations of macrorealism. We provide qualitative semiclassical reasoning for the numerical results involving a kicked top, and for two important initial states that behave very differently.

* manishd@imsc.res.in

† arul@physics.iitm.ac.in

I. INTRODUCTION

This paper aims to study the impact that chaos has on macrorealism, which is a set of assumptions proposed to test the limits of quantum mechanics. They codify the intuition of how macroscopic objects behave [1, 2] and are in direct contradiction to postulates of quantum mechanics when applied to macroscopic systems. These assumptions allow derivation of the Leggett-Garg (LG) inequalities and the no-signaling in time (NSIT) condition as found by Kofler and Brukner [3], which are necessary conditions for macrorealism to hold. While the Leggett-Garg inequalities are based on the results of sequential measurements in time, the NSIT conditions compare probability distribution of measurement outcomes with or without prior measurements. They also follow from the assumptions of macrorealism and can be violated even when the LG inequality is not.

Here we employ the NSIT condition to analyze whether quantized chaotic systems could be especially violative against the tests. As macrorealism is a test of correlations in time, it seems particularly fruitful to ask how the violations are sensitive to very different time evolutions, regular versus chaotic. The subject of macrorealism has been extensively studied lately in various directions; see [4] for a review, as well as [5–7]. Quantum chaos is seeing a surge of activity, with applications from many-body systems to black-hole physics. Newer techniques such as out-of-time-ordered correlators and operator scrambling to the eigenstate thermalization hypothesis have been developed (see [8] for a review). At a foundational level it could play an interesting role in explaining how one classical world emerges from all the unravelings of the decoherent histories of a multiverse [9]. Chaos, in the sense of a long time averaged positive Lyapunov exponent is seen as a classical property, and the differences between classical and quantum chaos are usually stark, and it is therefore of interest to explore how the assumptions of macrorealism fare in its presence.

Quoting Leggett from [2], macrorealism assumes that (1) “a macroscopic system with two or more macroscopically distinct states available to it will at all times be in one or the other of these states.” (2) “It is possible in principle to determine which of these states the system is in without any effect on the state itself or on the subsequent system dynamics.” (3) “The properties of ensembles are determined exclusively by initial conditions (and in particular not by final conditions)”. Kofler and Brukner have show that the NSIT condition, as discussed in detail below, follows from these assumptions [3]. The idea of macroscopic distinctness

is not uniquely defined and is reviewed in [10]. In this article we consider the disturbance due to projective measurements made by Alice on those made by Bob; the two canonical observers. We work with the well-studied kicked top [11–17], a generic Hamiltonian system with an integrable to chaotic transition. It is described by a large spin j object that is subject to both rotation and torsion in orthogonal directions. This is also a Floquet system in that the torsion is applied in periodic kicks, making the chaos possible as the dynamics is an area-preserving map of a sphere onto itself.

Previous related work in [18] involves a study of the LG inequality in a quantum nonlinear Kerr-like oscillator externally pumped by a series of ultrashort coherent pulses. They have shown the changes that accompany a regular-chaos transition in that system. There are some similarities between that study and this, both study a bosonic Floquet system. However, we study a finite dimensional system that is a textbook example of quantum chaos and has many experimental realizations. Most importantly we study a different version of macrorealism, NSIT, rather than the LG inequality.

A. Two measures of No-signaling in time

We want to study how much Alice’s measurement can affect Bob’s measurement. The question of how much disturbance is there however, immediately begs another question - when were the measurements made? Therefore, the study must necessarily get entangled with discussions of temporal separation between the measurements. Suppose that Alice and Bob measure observables $\mathbf{J} \cdot \hat{\mathbf{a}}$ and $\mathbf{J} \cdot \hat{\mathbf{b}}$ respectively, on a kicked top possessing total angular momentum j . Let t_0 be the initial time, and let Alice make her measurement at time t_α and Bob make his at t_β , with $t_0 < t_\alpha < t_\beta$.



Figure 1: The measurement timeline. Time increases along the axis towards right.

According to macrorealism, “a measurement does not change the outcome statistics of a later measurement” and is the no-signalling in time statement [3]. Its violation immediately implies that Bob’s unconditional (when Alice does not measure) and conditional probability (when Alice does measure) distributions are different.

Let $P(b, a; t_\beta, t_\alpha)$ be the joint probability distribution for Alice's and Bob's measurements described above. Here b is Bob's outcome and a is Alice's; t_β, t_α serve as parameters of the distribution, highlighting respective measurement times. Further, we define $P_B(b; t_\beta)$ as the unconditional probability for Bob's measurement of eigenvalue b at t_β and $P_C(b; t_\beta, t_\alpha)$ as the conditional probability for the same. It follows from the definition that

$$P_C(b; t_\beta, t_\alpha) = \sum_a P(b, a; t_\beta, t_\alpha), \quad (1)$$

and NSIT condition when cast into an equation, becomes

$$\forall t_\alpha < t_\beta : P_B(b; t_\beta) = P_C(b; t_\beta, t_\alpha) \quad (\text{true under MR}). \quad (2)$$

Alice makes only one measurement before Bob, and when Bob eventually compares the probability distributions he gets with and without the measurement, the results may be different. Since a good comparison should focus on both local and global features, we choose the following two complementary measures.

First is the standard Hellinger distance [19]. If we take N ordered pairs of events (x_i, y_i) with p_i (q_i) being the probability corresponding to x_i (y_i), then, the Hellinger distance between the distributions is defined as

$$H(p, q) = \frac{1}{\sqrt{2}} \sqrt{\sum_{k=1}^N (\sqrt{p_i} - \sqrt{q_i})^2}. \quad (3)$$

This distance is bounded between 0 and 1. Note that if and only if $p_i = q_i$ for each i , it is zero (a condition necessary and sufficient for violation of NSIT) and becomes maximum whenever $p_i = 1, q_j = 1; i \neq j$.

We consider another measure: the difference in how many values of $\mathbf{J} \cdot \hat{\mathbf{b}}$ could Bob have got in the two cases. This measure can be defined using the participation ratio. Suppose that p is a probability mass function for X which can take values $\{x_1, x_2, \dots, x_N\}$. Then

$$W(p) = \left(\sum_{k=1}^N p(x_k)^2 \right)^{-1} \quad (4)$$

is a good measure of how much the distribution p is spread, being bounded between 1 (when only one value is possible) and N (when all values are equally likely). We can compute it for P_B and P_C to get the accessible states. Then we can define

$$\Delta(P_C, P_B) = W(P_C) - W(P_B) \quad (5)$$

Regarding the temporal separation $t_\beta - t_\alpha$, in general Bob may choose to vary his measurement time from $t_\beta = 0$ to ∞ , according to an arbitrary probability distribution. Then, for a fixed t_β , Alice may choose to measure at any time before Bob, according to a probability distribution of her choice. Simplest examples would be the delta and the uniform distributions for both of them. We restrict the study to the following scenario:

- Alice measures at a fixed time interval before Bob (the delta distribution), and Bob's time is a uniform random variable in a range $(1, T)$.

This set up shall capture several features of interest.

II. MEASUREMENTS ON A KICKED TOP

Quantifying the disturbance in the spirit of NSIT condition, we shall make the said connection between chaos and macrorealism. The Hamiltonian generating the time evolution is taken to be the kicked top:

$$H(t) = J_y \frac{\pi}{2} + \frac{\kappa_0}{2j} J_z^2 \sum_{n=-\infty}^{\infty} \delta(t - n). \quad (6)$$

Here κ_0 is a parameter signifying the kick strength. The kicked top displays chaos in the classical limit $j \rightarrow \infty$ as κ_0 increases beyond 2 and becomes almost fully chaotic for $\kappa_0 > 6$. The corresponding quantum unitary map is the Floquet operator connecting states across a time-period (here chosen as unity) is given by

$$U = \exp(-i\kappa_0 J_z^2/2j) \exp(-iJ_y \pi/2) \quad (7)$$

which we shall often write as $U = TR$ where $T = e^{-i\kappa_0 J_z^2/2j}$ comes from the twist or torsion about the z axis and $R = e^{-iJ_y \pi/2}$ is rotation about the y axis.

As noted earlier, there is a major body of work concerning this “simple” dynamical systems, see the books by Haake [12] and Peres [13] including a cold atom experiment [15], and a transmon based one [16]. It has been used in studying the impact of chaos on entanglement [14, 17], and for small values of j it can be analytically solved and presents many intriguing features [17, 20] such as a proto-exponential growth of OTOC [21]. This system becomes increasingly macroscopic with increasing j , and therefore is relevant for the study of macrorealism tests.

Quantum mechanics intrinsically violates the assumptions of macrorealism. Therefore it is not a surprise that calculations would lead to violations of NSIT, especially for small j . To answer whether the degree of discord between the two depends on chaos or not, it is imperative to focus on identifying direct effects of chaos and filter out intrinsic violations arising from other known sources, such as incompatible measurements. Restricting to special initial states and measurement schemes will enable us to do so.

A. The conditional probability, connection to an OTOC, and the role of coherence

Here we consider what Alice's measurement does to the system, and discuss restrictions on $\hat{\mathbf{a}}, \hat{\mathbf{b}}$, the axes of measurements. Firstly, note that in calculating (1), Alice's action can be considered as a measurement that reduces the original pure state to a mixed state. To see this, let ρ_0 be the initial state and ρ_α be the state before Alice's measurement and suppose that the projectors of $\mathbf{J} \cdot \hat{\mathbf{a}}$ are $\{A_a\}$. Then

$$\sum_a A_a \rho_\alpha A_a \rho'_\alpha = \sum_a A_a \rho_\alpha A_a = \sum_a A_a U_\alpha \rho_0 U_\alpha^\dagger A_a \quad (8)$$

is the claimed mixed state post measurement. Here $U_\alpha = \exp(-iHt_\alpha)$ or U^{t_α} in the Floquet case. Subsequently, evolution occurs for $t_\beta - t_\alpha$, after which Bob measures $\mathbf{J} \cdot \hat{\mathbf{a}}$ whose projectors are $\{B_b\}$, and finds the distribution P_C :

$$P_C(b; t_\beta, t_\alpha) = \text{Tr} \left[U_{\beta\alpha} \rho'_\alpha U_{\beta\alpha}^\dagger B_b \right] = \sum_a \text{Tr} \left[U_{\beta\alpha} A_a \rho_\alpha A_a U_{\beta\alpha}^\dagger B_b \right]. \quad (9)$$

We use $U_{\beta\alpha} = \exp(-iH(t_\beta - t_\alpha))$ for the evolution operator from t_α to $t_\beta > t_\alpha$. In the case of Floquet operator U as we use in this work $U_{\beta\alpha} = U^{t_\beta - t_\alpha}$, where these times are integers. Multiply and divide by $\text{Tr}[\rho_\alpha A_a]$ for each term in the sum, to get

$$P_C(b; t_\beta, t_\alpha) = \sum_a \text{Tr} \left[U_{\beta\alpha} \rho_\alpha U_{\beta\alpha}^\dagger B_b \right] \text{Tr}[\rho_\alpha A_a]$$

where $\rho_a = A_a \rho_\alpha A_a / \text{Tr}[\rho_\alpha A_a]$. This is of course $\sum_a P(b, a; t_\beta, t_\alpha)$, and is the same as (1). The unconditional probability is simply $P_B(b; t_\beta, t_\alpha) = \text{Tr} \left(U_{\beta\alpha} \rho_0 U_{\beta\alpha}^\dagger B_b \right)$.

We now observe that the conditional probability is one the simplest forms of an out-of-time-ordered correlator or OTOC. Let $U_\alpha^\dagger A U_\alpha = A(t_\alpha)$ be the Heisenberg evolution of the projector over the times t_α . Using such Heisenberg evolved projection operators, it is simple

to then rewrite Eq. (9) as

$$P_C(b; t_\beta, t_\alpha) = \text{Tr} [\rho_0 A_a(t_\alpha) B_b(t_\beta) A_a(t_\alpha)]. \quad (10)$$

This is the simplest form of an OTOC as the times are ordered non-monotonically. It has been referred to as a 3-OTOC and used in [22, 23] where it has been shown it play an important role in the growth of the norm of commutator. This quantity has not been nearly as much studied as the 4-point OTOC, but it is clear that this is related to the conditional probability. In fact OTOC has also been studied as a measure of “disturbance” and has been pressed into service to elucidate the so-called “quantum butterfly effect”, see [24] for a recent review.

Next, we note that measurements of non-commuting operators $\mathbf{J} \cdot \hat{\mathbf{a}}, \mathbf{J} \cdot \hat{\mathbf{b}}$ will give violations that typically would get amplified in time, but may have nothing to do with the dynamics itself. To see this possibility, specialize to no evolution. Let the initial state be an eigenstate of $\mathbf{J} \cdot \hat{\mathbf{b}}$. If $\hat{\mathbf{a}} \neq \hat{\mathbf{b}}$, Bob’s measurement will change the state from what Alice’s measurement had reduced it to, and thereby create a difference in P_B and P_C . Any bonafide distance we use will give non-zero value in their comparison. Even when system evolves, this effect persists because of continuity. Origin of this violation lies in the fact that $[\mathbf{J} \cdot \hat{\mathbf{a}}, \mathbf{J} \cdot \hat{\mathbf{b}}] \sim \hat{\mathbf{a}} \times \hat{\mathbf{b}}$ and not in chaos. Avoiding such violation would decrease noise, and hence allow a better understanding of the effects that do arise from chaos. Therefore, we restrict to $\hat{\mathbf{a}} = \hat{\mathbf{b}}$ case, and henceforth work with density matrices in the $\mathbf{J} \cdot \hat{\mathbf{a}}$ eigenbasis $\{|\hat{\mathbf{a}}, m\rangle\}$.

As there is now a preferred basis for both the measurements, the density matrix is best expressed in this basis. The origin of violations for such cases lies in the removal of off-diagonal terms from the density matrix, because of Alice’s measurement. To see this, suppose $\rho_\alpha = \sum_{m,n} \varrho_\alpha^{mn} |\hat{\mathbf{a}}, m\rangle \langle \hat{\mathbf{a}}, n|$ is the expansion of the state before Alice’s measurement and let $A_k = |\hat{\mathbf{a}}, k\rangle \langle \hat{\mathbf{a}}, k|$. Then post measurement,

$$\rho'_\alpha = \sum_k A_k \rho_\alpha A_k = \sum_{m,n,k} \varrho_\alpha^{nm} \delta_{km} \delta_{nk} |\hat{\mathbf{a}}, k\rangle \langle \hat{\mathbf{a}}, k| = \sum_k \varrho_\alpha^{kk} A_k. \quad (11)$$

Note that the diagonal terms are unchanged. Therefore, deletion of off-diagonals leads to all the observed differences between P_B and P_C . As time evolves, these non-diagonal entries effect the probabilities of measurement, because states evolves via conjugation by U . The off-diagonal elements measure the quantum coherence of the state, and this is a known

resource for quantum information. While measurement destroys this coherence, dynamics restores it, and the NIST is a measure of this competition.

Motivated by this, we consider the l_1 norm of coherence [25]

$$C_A(t_\alpha^-) = \sum_{k \neq m} |\varrho_\alpha^{km}| \quad (12)$$

as a measure of disturbing power, because it measures strength of the off-diagonals in the matrix at time t_α^- , just before Alice's measurement. Here A in the subscript denotes the basis chosen by her. When it is zero, Alice causes no disturbance, and when it is large, intuitively, her measurement becomes more destructive. As κ_0 increases, C_A accentuates for initially localized states because of the non-trivial action of twist operator T (discussed in appendix). This leads to increased violation due to Alice's measurement, which is seen in the results below.

B. Role of time between measurements

As we are dealing with a discrete time dynamics, all times such as t_α and t_β are now integers. Alice and Bob decide on $t_\beta - t_\alpha = n$, where Bob's time of measurement t_β is a uniform random variable over the set $\{n, n+1, \dots, n+T\}$. As a result, any distance computed between P_B and P_C which depends on t_β is another random variable. For a distance function $d(t_\beta, t_\alpha)$, we define $d_n(t_\beta) \equiv d(t_\beta, t_\beta - n)$, whose average is given by [26]:

$$\langle d_n \rangle = \frac{1}{T+1} \sum_{t_\alpha=0}^T d_n(n+t_\alpha). \quad (13)$$

Here d may be H or Δ , with $T \gg 1$. In the following, we study this average as a function of κ_0 for two special initial states which are coherent states. In the kicked top the coherent state $|\hat{\mathbf{y}}, j\rangle$ corresponds to a fixed point in the classical map, and $|\hat{\mathbf{z}}, j\rangle$, is part of a period-4 cycle.

Being coherent [27, 28], they come closest to points in the phase space, which are classical states. Further, they both display quantum signatures of chaos [17] when corresponding classical orbits lose stability with increase in κ_0 . Therefore, they are good examples for studying effects of chaos in Δ and H . We push their further discussion to the appendix for clarity. We set $\hat{\mathbf{a}} = \hat{\mathbf{b}} = \hat{\mathbf{z}}$ in the following and also $j = 15$ as a reasonably large system size. We briefly discuss the generalization for other values of j .

Even-odd n differences in J_z measurements

If Alice and Bob both measure J_z , the violations recorded in Δ and H are critically dependent on whether n , the time between measurements, is even or odd, especially at small values of κ_0 . As an extreme case, at $\kappa_0 = 0$, we see that for odd n , Δ and H are non-zero (Fig. 2 shows the case for Δ), whereas for even n , both are zero. This happens

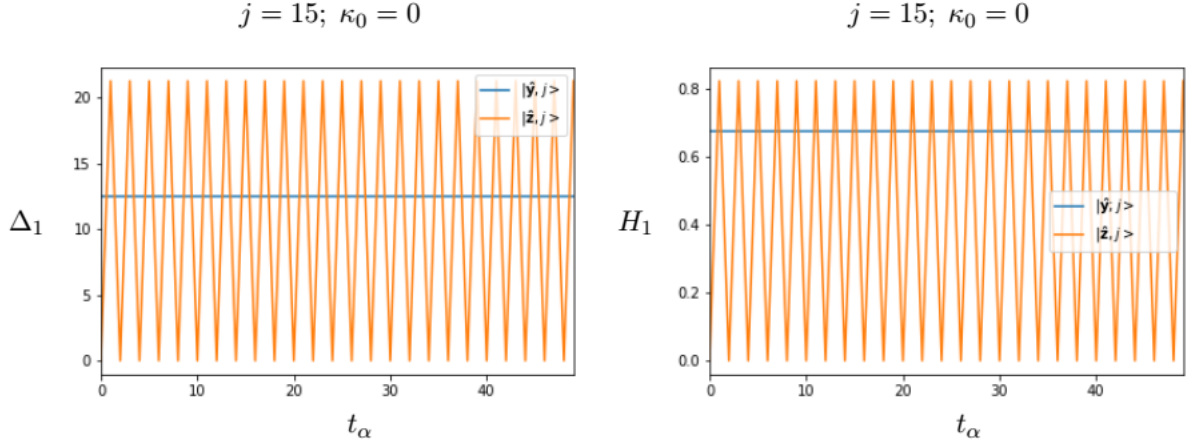


Figure 2: The distances Δ_1 and H_1 , for $n = 1$ in the absence of chaos: $\kappa_0 = 0$, as a function of Alice's measurement time t_α . The constant line is for the initial state $|\hat{\mathbf{y}}, j\rangle$, while the oscillatory curve vanishing for even t_α is for the initial state $|\hat{\mathbf{z}}, j\rangle$. Due to continuity, this effect persists for small non-zero values of κ_0 as well.

because of the specific initial states and measurement axis. When $\kappa_0 = 0$ the state $|\hat{\mathbf{z}}, j\rangle$ evolves to give the 4-cycle as the dynamics is simply R , rotation by $\pi/2$ about the y -axis:

$$|\hat{\mathbf{z}}, j\rangle \rightarrow |\hat{\mathbf{x}}, j\rangle \rightarrow |\hat{\mathbf{z}}, -j\rangle \rightarrow |\hat{\mathbf{x}}, -j\rangle \quad (\text{repeat}). \quad (14)$$

At even t_α , state returns to a J_z eigenstate and hence Alice's measurement creates no effect. These cases correspond to zero values seen in Fig. 2. At odd t_α however, she produces mixture of J_z eigenstates, which is invariant under R^2 . If then Bob measures at even t_β , so that n is odd, what would have been a J_z eigenstate for him without the measurement, becomes a mixture too. These cases correspond to the maxima seen in Fig. 2. For even n and odd t_α , using the fact that measurement axis is common and that mixtures produced are symmetric under R^2 , it follows that $\Delta, H = 0$. For initial state $|\hat{\mathbf{y}}, j\rangle$, there is no evolution for $\kappa_0 = 0$. Thus, Alice's measurement can only reduce it to one mixed state which is again

invariant under R^2 , but changes under R . Again, as a result, odd n give violation, whereas even n do not. This time however, there are no oscillations as t_β varies.

Therefore even in plain rotation (when there is no chaos), we see significant violation of NSIT for odd n values. This effect, by continuity, persists even when κ_0 increases, and for the purposes of establishing a connection between chaos and the signaling, it is unwanted. Therefore, we turn our attention to only even n for both the states.

C. Results for initial states $|\hat{\mathbf{z}}, j\rangle$ and $|\hat{\mathbf{y}}, j\rangle$ when $\kappa_0 \neq 0$

Figure 3 shows results for the average of Δ_n and H_n when the initial state is $|\hat{\mathbf{z}}, j\rangle$ for a few values of even n . It is seen that a nearly linear growth is observed in both quantities with a growing slope as n increases. The NSIT violation plateaus in both quantities when κ_0 is between 3 and 4, beyond which the variations between different n are lost. Physically, it means that if there is strong mixing, on average it doesn't matter how long ago Alice measured on the system. Her measurement causes an equally powerful effect, provided, she measures even periods before Bob. The disturbance due to Alice's measurement leads to an enlargement in Bob's outcome possibilities, on an average. As a result we observe that $\langle W(P_C) \rangle > \langle W(P_B) \rangle$, this in fact is seen in all the cases we have studied and needs further exploration. The 4-period cycle corresponding to this state undergoes a change of stability at $\kappa_0 = \pi$. We identify the saturation-like behavior in κ_0 as a consequence of this loss of stability.

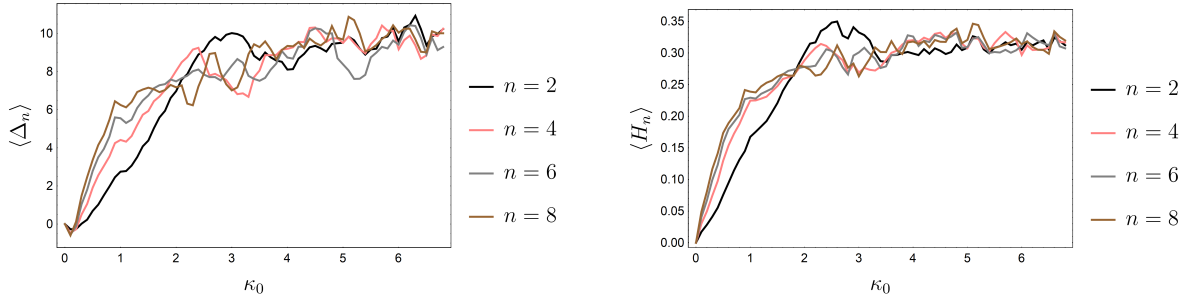


Figure 3: The distances Δ_n and H_n , averaged over $T = 50$ initial times t_α . For the initial state $|\hat{\mathbf{z}}, j\rangle\langle\hat{\mathbf{z}}, j|$, $j = 15$, Alice measures J_z at t_α while Bob measures J_z at $t_\alpha + n$.

Figure 4 shows the results when the initial state is $|\hat{\mathbf{y}}, j\rangle$. A similarity with the $|\hat{\mathbf{z}}, j\rangle$ case is seen, in as much as there is a growth of the NSIT distance measures as a function of κ_0

and a saturation that corresponds to the onset of classical chaos. The saturation values are approximately the same. However there are two evident differences. (i) The point where the functions saturate is at a smaller value around $\kappa_0 = 2$. As mentioned the classical point corresponding to the initial state is a fixed point which loses its stability at $\kappa_0 = 2$, which corresponds well to the parameter at which macrorealism indicators also saturate. (ii) There is a prominent overshoot of these functions before the saturation. The overshoot gets sharper as the time between the measurements increases.

The second difference is worth discussing further and advance possible causes for it. First, notice that these are averages taken over the first 50 starting times for Alice's measurement from t_α from 0 to 50, therefore these are rather large violations. The maximum violations will occur when Alice's measurement results states that are very different from those produced without her actions. That the measurements happen in the J_z basis, implies that the post-measurement states are an ensemble of J_z eigenstates that under the kicked top for small κ_0 are restricted to the $x - z$ plane, while without Alice's measurement the state would still have been an approximate J_y eigenstate as the initial state is on a stable fixed point. Thus the resultant states fare very different under J_z measurements. This is a qualitative heuristic reasoning that may explain that the larger violations do not seem to happen after the onset of chaos.

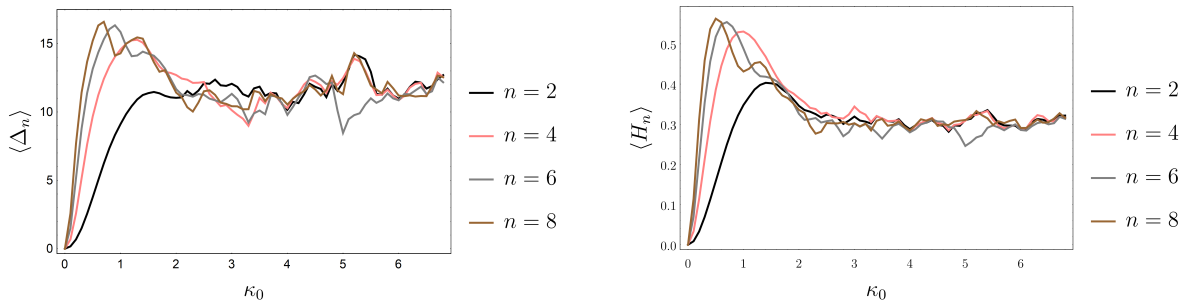


Figure 4: Same as the previous figure, except that the initial state is $\rho_0 = |\hat{\mathbf{y}}, j\rangle\langle\hat{\mathbf{y}}, j|$. Several features are as they were in the case of $|\hat{\mathbf{z}}, j\rangle$. Note however, that the peaks occur around $\kappa_0 = 2$ where the fixed point loses its stability. For small κ_0 , the prominent difference for different n values arises because of time evolution for the state localized in the regular region.

We have not shown so far what happens when $\kappa_0 > 0$ and the time between Alice's and Bob's measurements is an odd integer. Figure 5, shows this as it includes all intervals from

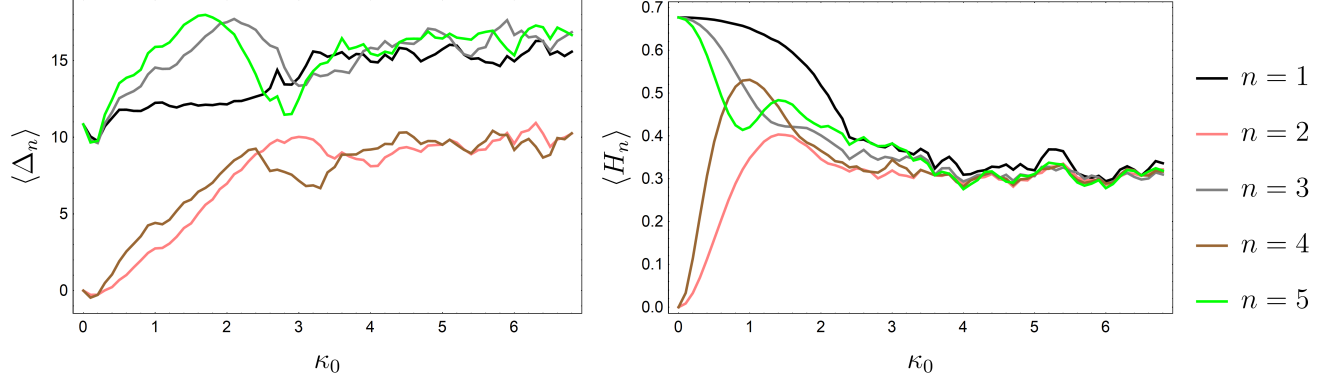


Figure 5: The distance measures are shown including odd and even intervals in the range $1 \leq n \leq 5$. for the initial state $|\hat{\mathbf{z}}, j\rangle$ (left) the odd/even effect persists well into the fully chaotic regime. For the $|\hat{\mathbf{y}}, j\rangle$ case (right), for low κ_0 values, the proximity to rotation about the y -axis produces the difference which vanishes with the onset of chaos.

1 to 5. The differences seen arise because of the special nature of the states and the axis of measurement. For small values of κ_0 the rotation dominates over the torsion. However, it is interesting and surprising to note that in the case of the initial state being $|\hat{\mathbf{z}}, j\rangle$ the system has not “forgotten” even when κ_0 is very large and is deep in fully chaotic regime. This indicates that the type of states that result with measurements and chaos can be quite different from random states. In contrast when the initial state is $|\hat{\mathbf{z}}, j\rangle$, odd and even time intervals do not matter when there is global chaos. Note that in this figure different measures are used in for the two cases, but this is not essential, as they are qualitatively identical.

Figure 6 shows the contour plots corresponding to the time averaged plots in figure ?? . Note that in (a) the oscillatory behaviour in Δ is lost for $\kappa_0 > \pi$. Similar effect is seen in (b), where oscillations become less prominent beyond this point. Both the results highlight that system tends to forget the sharp distinction between even t_α and odd t_α because of chaos, which exists from $\kappa_0 \sim 1$ to 3.

The preceding results were all for $j = 15$ with 31 states, and it is of interest to see the dependence on this, as the classical limit is effectively reached when $j \rightarrow \infty$. Shown in Fig. 7 is a scaled quantity $v_\Delta = \langle \Delta_2(\kappa_0 = 7) \rangle / (2j + 1)$ and $v_H = \langle H_2(\kappa_0 = 7) \rangle$ as j is varied. The parameter κ_0 is fixed at a value when classical chaos is dominant, and again the two distinct initial states are examined. Roughly, the degree of violation is seen to increase with j and tends to a constant at surprisingly small values of j 4 – 5. Note that in the

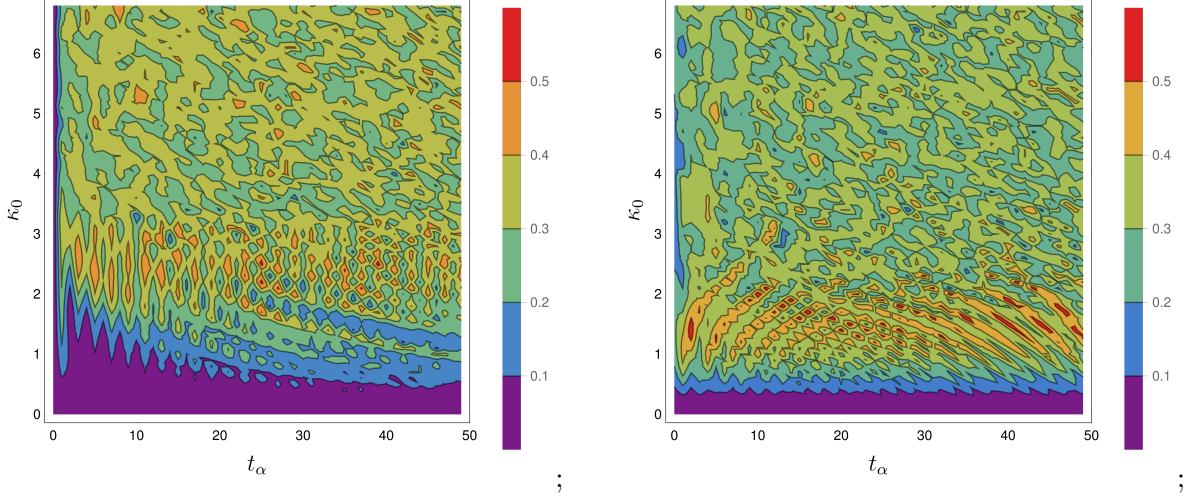


Figure 6: Contour plot of Δ_2 , as a function of the time of Alice's measurement, t_α and the parameter κ_0 which controls chaos. Shown are the cases when the initial state is $|\hat{\mathbf{z}}, j\rangle$ (left) and $|\hat{\mathbf{y}}, j\rangle$ (right). Note the change in behavior of oscillations beyond $\kappa_0 \sim \pi$ on the left, and the change at $\kappa_0 \sim 2$ on the right. The odd-even effects are seen as oscillations that are especially visible in the left plot.

kicked top Floquet operator, the torsion term contains the ratio κ_0/j and hence for very small j , increasing κ_0 will show periodicity and not reflect classical chaos. Thus for as small angular momenta as $j = 3/2$ and $j = 2$ the kicked top is exactly solvable [17] but does not reflect the classical dynamics beyond about $\kappa_0 = 3$, when chaos just sets in. It is well-known that the kicked top can be considered as an all-to-all interacting system of $2j$ qubits, see for example [29]. Thus full fledged chaos effects can be felt only for j that is of the order of ~ 10 , although it has also been shown that even for small value of j or number of qubits, the system already exhibits some signatures of chaos [21] or instability such as exponential growth of OTOC, albeit for a very small time. Thus it seems reasonable that for $\kappa_0 = 7$, the NSIT measures tend to saturate for $j \approx 10$, although in the Δ measure it seems to matter what the initial state is. As preliminary results, these indicate that in a closed system with unitary dynamics, the classical limit does not imply that the NSIT will become increasingly valid.

We note that these results are linked consistently with results from quantum chaos. If one starts from a coherent state, it gets stretched and folded due to the unstable and stable manifolds in a chaotic system, and leads to delocalization along with superpositions.

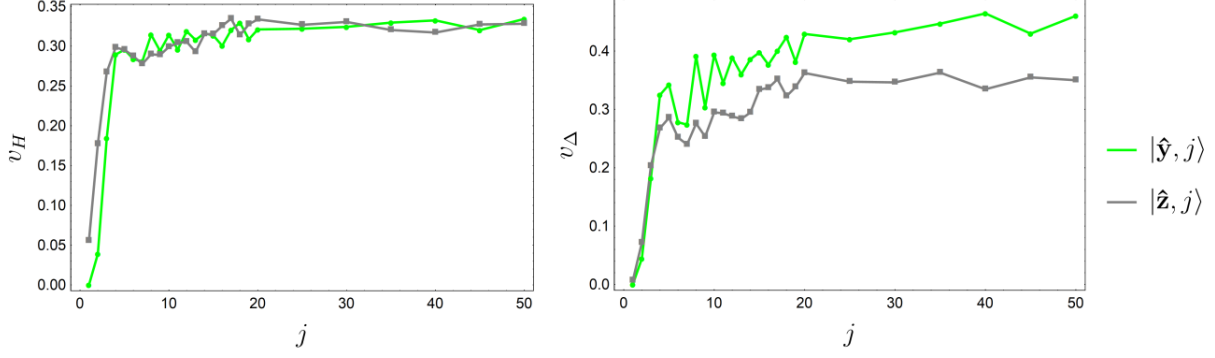


Figure 7: The time averaged violation due to measurement for complete chaos) ($\kappa_0 = 7$) as a function of j . Here $t_\beta - t_\alpha = n = 2$ here, but this holds for all even n as was shown in the case of $j = 15$ above.

This is in direct contradiction with the first assumption of macrorealism, because it allows a faster and more prominent superposition between macroscopically distinct quantum states. More quantitatively, quantum chaotic systems have a much earlier time at which quantum effects set in than regular systems: as the Ehrenfest time [30–32] at which quantum-classical correspondence breaks down scales as $-\log(\hbar)/\lambda$, where \hbar is a scaled Planck constant, scaled by a characteristic action of the system, and λ is the Lyapunov exponent, whereas in regular systems this time is much larger and scales $\hbar^{-1/2}$.

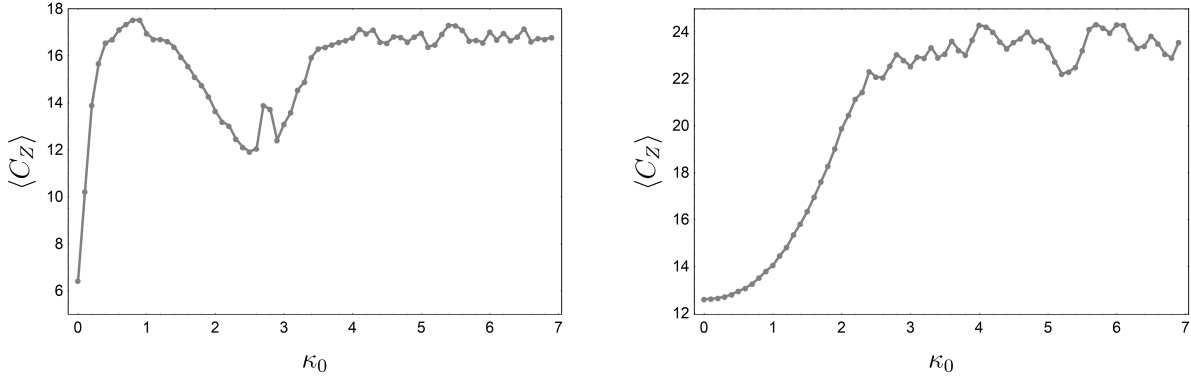


Figure 8: The coherence $C_Z(\rho)$ in Eq. (12) is shown as an average over the first 50 time steps for $|\hat{\mathbf{z}}, j\rangle$ (left) and $|\hat{\mathbf{y}}, j\rangle$ (right) initial states. Note the difference in the vertical axis scales between the two figures. The large value of coherence at $\kappa_0 = 0$ in the second case is due to the large J_z coherence for a J_y eigenstate.

Finally we calculate the coherence in the state just before Alice's measurement as in-

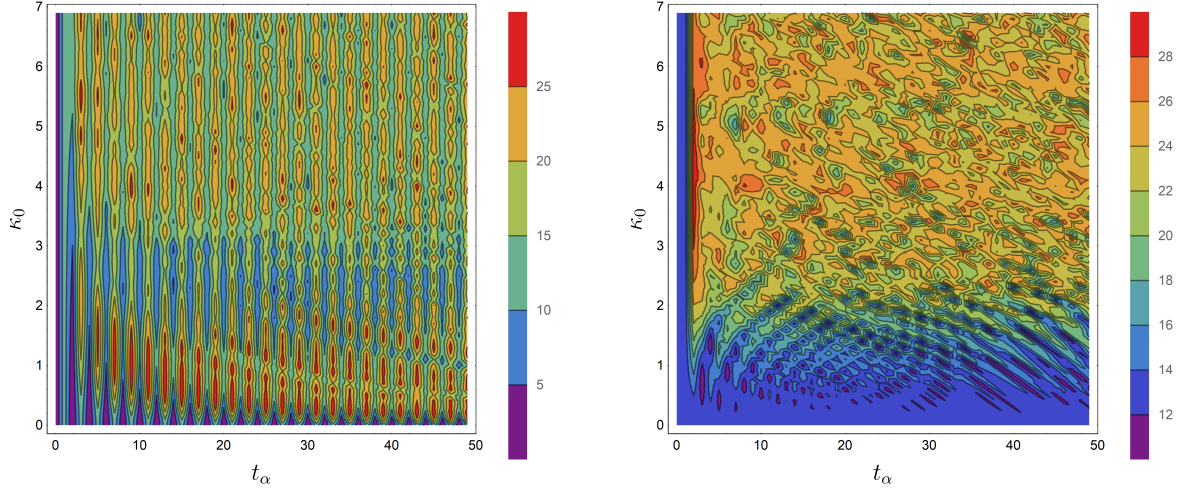


Figure 9: Contour plots of the coherence C_Z as a function of the time at which Alice measures and the parameter κ_0 are shown here for the two initial states, $|\hat{\mathbf{z}}, j\rangle$ (left) and $|\hat{\mathbf{y}}, j\rangle$ (right). The correspondence with plots showing NSIT violations as in Fig. 6 are noted.

indicated in Eq. (12). Figure 8 shows the coherence measure C_Z for the two initial states as a function of the parameter κ_0 . The coherence is found at $0 \leq t_\alpha \leq 50$ and averaged. The 4-period cycle associated with it is stable whenever $(2 \cos \kappa_0 + \kappa_0 \sin \kappa_0)^2 < 4$. As a result, in the interval $[0, 7]$ there are 4 points where the stability of cycle changes. These are $\kappa_0 = 0, \pi, \sim 5.6$ and 2π . Till $\kappa_0 \sim 1$, the cycle remains enclosed in a narrow separatrix region, and the at odd times gets predominantly rotated close to a J_x eigenstate which has a large coherence in the J_z basis. But with increasing κ_0 further, these states have lesser overlaps with J_z eigenstates and leads to a lower coherence. Beyond about $\kappa_0 = \pi$, the cycle loses stability and the coherence increases and saturates. Beyond 4, chaos becomes quite prominent over the whole sphere, and the windows of stability become smaller and does not impact the quantum for these small values of j . We notice that in the case of the J_y eigenstate, the coherence shows a smooth and monotonic increase and beyond $\kappa_0 = 2$ saturates. However, notice that the scales in the two plots are different and hides the large coherences that are present in this second case, simply because of the initial state being uniformly close to that of an J_y eigenstate. This large coherence could be connected with the large violations of the NSIT in these cases, but this needs further investigation. The smoothness of the increase also reflects the much simpler classical structure that is far from

any separatrix for this initial state. Figure 9 shows the coherence as a function of time and the parameter κ_0 , without any averaging. These show very similar patterns to those for the NSIT measures in Fig. 6, and the influence of coherence on these measures could be explored further, for example as the coherences evolved between the measurements.

III. SUMMARY AND DISCUSSIONS

We studied violations of macrorealism via the no-signaling in time condition for a paradigm quantum chaotic system, the kicked top. Introducing two measures of the violations we have mainly studied numerically their dependence on the chaos parameter and the time between the measurements. We have shown that there is a strong parity effect in the time between measurements that persists quite into the chaotic regimes for certain states. We have shown how the NSIT violations can be very different for different initial states and have also provided qualitative reasoning for these based on semiclassical or classical settings. While there is no simple rule such as larger chaos implies larger NSIT violations, there is a fair amount of correlations and it is true that chaos engenders a large NSIT violation. The role of the stability of periodic orbits in the NSIT violations is clearly seen, and when the classical and quantum dynamics is stable, generic states can lead to smaller values of violation. Although there could be special states that can behave differently. We have seen that these cases have to do with the presence of a large coherence in the measurement basis. Thus these may be exceptional, but again point to a direction for further investigations and connections between quantum coherence and macrorealism conditions.

We have also observed that the NSIT correlations are a form of a an out-of-time-ordered correlator, a 3-OTOC. The OTOC is a sensitive measure of quantum chaos and instability, and a quantum Lyapunov exponent has been defined with these. Thus the connection is intriguing and deserves more exploration. We highlighted that in a general case, a combination of factors is responsible for the overall violation, one of them being measurement of non-commutative operators in our Alice-Bob setup. Although the details may in general depend on initial state and n , the time between measurements, in the presence of chaos we showed that long-time average of disturbances is largely independent of the exact value of n in the chaotic limit. The dynamics can lead to formation of different equivalent sets of n values, within which these differences almost completely vanish. Finally, the variation

of disturbance as a function of j shows that effects of chaos are more potent for larger j , which implies that chaotic systems are the among the best places to study properties such as macroscopic coherence and tests of macrorealism.

ACKNOWLEDGMENTS

We would like to thank Dipankar Home for generous email discussions on an earlier version of this work.

APPENDIX: SOME ASPECTS OF CLASSICAL AND QUANTUM DYNAMICS OF THE KICKED TOP

Here we review the classical limit, focusing on the chosen initial states, followed by study of their quantum evolution. The latter explains how an increase in κ_0 leads to an increase in $C_A(\rho)$ for localized states.

A. Classical Map

Taking the limit of $j \rightarrow \infty$ in (6) with $J = \sqrt{j(j+1)}$ gives us the classical Hamiltonian. If we think of the classical vector \mathbf{J} in spherical polar coordinates, so that

$$\mathbf{J}/J = (\sin \theta \cos \phi, \sin \theta \sin \phi, \cos \theta), \quad (15)$$

solving the Hamilton's equations (taking $q = \phi$, $p = \cos \theta$) it is easily seen that the δ kick is an impulsive rotation of \mathbf{J} about z axis by an angle $J_z \kappa_0$, where $J_z = J \cos \theta$. During the kick, the rotation bit of Hamiltonian is negligible and thus Hamilton's equation integrates to give

$$\phi(n^+) - \phi(n^-) = \int_{n^-}^{n^+} dt \dot{\phi} = \int_{n^-}^{n^+} dt \frac{\partial H}{\partial p} = J \kappa_0 \cos \theta \int_{n^-}^{n^+} dt \sum_{-\infty}^{\infty} \delta(t - k) = J_z \kappa_0 \quad (16)$$

for any n . Therefore, we see that this system is rotating about two axes in each turn; by a constant angle of $\frac{\pi}{2}$ around the y axis, and by a variable angle around the z -axis. This "variation" in the angle is a necessary ingredient of chaos.

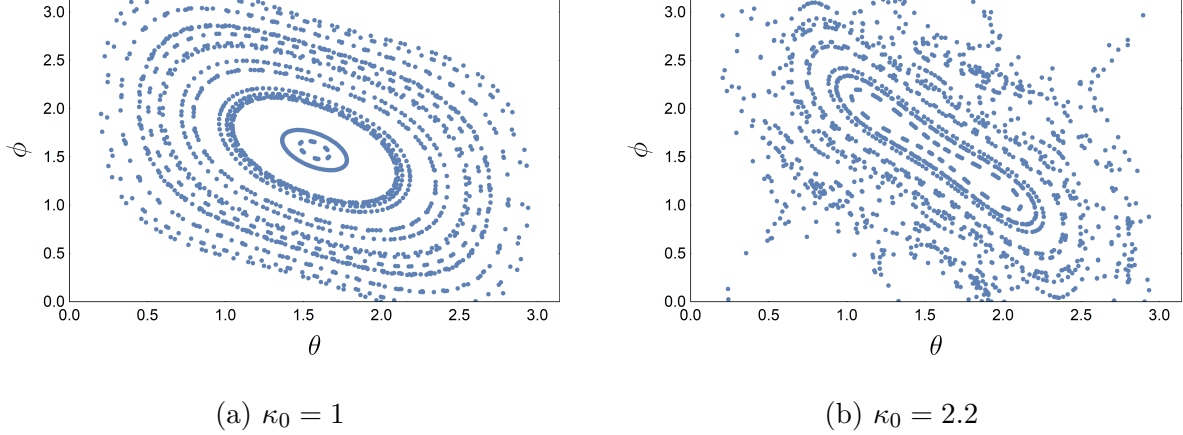


Figure 10: Phase space trajectories in the vicinity of fixed point at $Y = 1$ for two different cases, on the left, motion is quite regular whereas on the right, the bifurcation at $\kappa_0 = 2$ has created instability.

This system evolves according to a 2D map - because \mathbf{J}^2 is a constant of the motion - which is

$$X_i = Z_{i-1} \cos(\kappa_0 X_{i-1}) + Y_{i-1} \sin(\kappa_0 X_{i-1}) \quad (17)$$

$$Y_i = -Z_{i-1} \sin(\kappa_0 X_{i-1}) + Y_{i-1} \cos(\kappa_0 X_{i-1}) \quad (18)$$

$$Z_i = -X_{i-1} \quad (19)$$

where $X, Y, Z = J_{x,y,z}/j$, and obey $X^2 + Y^2 + Z^2 = 1$ [11]. These equations can be obtained from Heisenberg's equations of motion in the classical limit. The fixed points at the poles $Y = \pm 1$ and the equatorial 4 period cycle $Z = 1 \rightarrow X = 1 \rightarrow Z = -1 \rightarrow X = -1$ are of special relevance to us; each of these exists for all κ_0 values. In the quantum case, these fixed points and this cycle correspond to $|\hat{\mathbf{y}}, \pm j\rangle$ and $|\hat{\mathbf{z}}, j\rangle$ respectively.

As κ_0 increases, new fixed points and cycles are born, and on further increase, they become unstable, to bifurcate into new fixed points and cycles. The game starts at $\kappa_0 = 2$, when the fixed points at $Y = \pm 1$ lose their stability, giving rise to two new FPs. Figure 10 shows the trajectories near $Y = 1$ as κ_0 changes from 1 to 2.2. By $\kappa_0 = 3$, most of the sphere becomes chaotic, but there are some significant islands of stability, notably the ones around new fixed points and one around the 4 period cycle mentioned above, which loses stability at π ; it is stable whenever $(2 \cos \kappa_0 + \kappa_0 \sin \kappa_0)^2 < 4$. At $\sqrt{2}\pi \sim 0.442$, these FPs become unstable as well. By $\kappa_0 = 6$, system is essentially fully chaotic. See [11, 12] for details.

B. Quantum Dynamics

1. Dynamics for initial state $|\hat{\mathbf{z}}, j\rangle$

We will find it convenient to move back and forth between the J_z and J_x basis. From (7) it follows that the projectors $Z_m = |\hat{\mathbf{z}}, m\rangle \langle \hat{\mathbf{z}}, m|$ and $X_m = |\hat{\mathbf{x}}, m\rangle \langle \hat{\mathbf{x}}, m|$ obey

$$TZ_mT^{-1} = Z_m; \quad R^2Z_mR^{-2} = Z_{-m}; \quad RZ_mR^{-1} = X_m; \quad RX_mR^{-1} = Z_{-m}. \quad (20)$$

Note that for $\kappa_0 = 0$, the dynamics is trivial. We have a rotating vector starting on Z_j , which goes to the J_x eigenstate X_j , followed by Z_{-j} and finally back to X_j , completing the cycle. For small but non-zero κ_0 , $T \neq 1$. Simplifying TX_jT^{-1} by using Baker-Hausdorff formula, [33]

$$TX_jT^{-1} = X_j - \frac{i\kappa_0}{2j}[J_z^2, X_j] - \frac{\kappa_0^2}{4j^2}[J_z^2, [J_z^2, X_j]] \cdots \quad (21)$$

Using $K_{\pm} = J_y \pm iJ_z$, in analogy to standard raising and lowering operators, after some calculations, one finds

$$[J_z^2, X_j] = \frac{1}{2}\sqrt{j(2j-1)}(|\hat{\mathbf{x}}, j\rangle \langle \hat{\mathbf{x}}, j-2| - |\hat{\mathbf{x}}, j-2\rangle \langle \hat{\mathbf{x}}, j|) \quad (22)$$

and $[J_z^2, [J_z^2, X_j]]$ carries terms like $X_{j-2}, X_j, |\hat{\mathbf{x}}, j-2\rangle \langle \hat{\mathbf{x}}, j|, |\mathbf{x}, j\rangle \langle \hat{\mathbf{x}}, j-4|$.

For small κ_0 , we may neglect the higher order terms, to conclude that operation of T produces some off diagonal terms and mixes X_j with nearby states. Because the “ladder” is at an end for $m = j$, we only got the lower state X_{j-2} , but for $m \neq \pm j$, we do get neighbours on both sides. Note that the immediate neighbours are not mixed in the process.

After a rotation, $X_m \rightarrow Z_{-m}$. The off-diagonal J_x terms also rotate, in a sense. Note that $R^4 = \pm 1$, and the fact that R cannot distinguish between z axis and x axis. It can only do a counter-clock rotation by $\pi/2$ of each of their eigenstates, giving the same phase ϕ_m for X_{\pm} and Z_{\pm} , if any. Therefore,

$$R|\hat{\mathbf{x}}, m\rangle \langle \hat{\mathbf{x}}, n|R^{-1} = \phi_{mn}|\hat{\mathbf{z}}, m\rangle \langle \hat{\mathbf{z}}, n|. \quad (23)$$

Torsion does nothing to the Z 's, whereas the off-diagonal J_z terms again pick up opposite phases, but clearly, the magnitude of the off-diagonal is not affected. This explains how the coherence (12) increases in both J_z and J_x basis with increase in κ_0 .

As κ_0 increases, the higher order terms become relevant and as a result the mixing becomes stronger. For such cases, a single kick can mix several $\{X_m\}$ states.

2. Dynamics for $|\hat{\mathbf{y}}, j\rangle$

Defining $Y_m = |\hat{\mathbf{y}}, m\rangle\langle\hat{\mathbf{y}}, m|$, it follows from (7) that

$$RY_mR^{-1} = Y_m; \quad \bar{R}X_m\bar{R}^{-1} = Y_m; \quad TY_mT^{-1} = \bar{R}(TX_mT^{-1})\bar{R}^{-1} \quad (24)$$

where $\bar{R} = \exp(-iJ_z\pi/2)$. For $\kappa_0 = 0$, the state is invariant because it is an eigenstate of R . For $\kappa_0 > 0$, it is clear that behavior is similar to what we had before. The action of T on Y_m is just like its action on X_m 's, and mixes neighbouring states in J_y basis too. Of course, this should be expected from symmetry between x and y axes with respect to z axis.

-
- [1] A. J. Leggett and Anupam Garg. Quantum mechanics versus macroscopic realism: Is the flux there when nobody looks? *Phys. Rev. Lett.*, 54:857–860, Mar 1985.
 - [2] A J Leggett. Testing the limits of quantum mechanics: motivation, state of play, prospects. *Journal of Physics: Condensed Matter*, 14(15):R415–R451, apr 2002.
 - [3] Johannes Kofler and Časlav Brukner. Condition for macroscopic realism beyond the leggett-garg inequalities. *Phys. Rev. A*, 87:052115, May 2013.
 - [4] Clive Emary, Neill Lambert, and Franco Nori. Leggett–garg inequalities. *Reports on Progress in Physics*, 77(1):016001, dec 2013.
 - [5] Lucas Clemente and Johannes Kofler. Necessary and sufficient conditions for macroscopic realism from quantum mechanics. *Phys. Rev. A*, 91:062103, Jun 2015.
 - [6] Lucas Clemente and Johannes Kofler. No fine theorem for macrorealism: Limitations of the leggett-garg inequality. *Phys. Rev. Lett.*, 116:150401, Apr 2016.
 - [7] J. J. Halliwell. Comparing conditions for macrorealism: Leggett-garg inequalities versus no-signaling in time. *Phys. Rev. A*, 96:012121, Jul 2017.
 - [8] Luca D’Alessio, Yariv Kafri, Anatoli Polkovnikov, and Marcos Rigol. From quantum chaos and eigenstate thermalization to statistical mechanics and thermodynamics. *Advances in Physics*, 65(3):239–362, 2016.
 - [9] Philipp Strasberg, Teresa E. Reinhard, and Joseph Schindler. First principles numerical demonstration of emergent decoherent histories. *Phys. Rev. X*, 14:041027, Oct 2024.
 - [10] Florian Fröwis, Pavel Sekatski, Wolfgang Dür, Nicolas Gisin, and Nicolas Sangouard. Macroscopic quantum states: Measures, fragility, and implementations. *Rev. Mod. Phys.*, 90:025004,

May 2018.

- [11] F. Haake, M. Kuś, and R. Scharf. Classical and quantum chaos for a kicked top. *Zeitschrift für Physik B Condensed Matter*, 65(3):381–395, Sep 1987.
- [12] F. Haake. *Quantum Signatures of Chaos*. Springer-Verlag, Berlin, 1991.
- [13] Asher Peres. *Quantum Theory: Concepts and Methods*. Kluwer Academic Publishers, New York, 2002.
- [14] Shohini Ghose and Barry C. Sanders. Entanglement dynamics in chaotic systems. *Phys. Rev. A*, 70:062315, 2004.
- [15] S. Chaudhury, A. Smith, B. E. Anderson, S. Ghose, and P. S. Jessen. Quantum signatures of chaos in a kicked top. *Nature*, 461:768, 2009.
- [16] C. Neill, P. Roushan, M. Fang, Y. Chen, M. Kolodrubetz, Z. Chen, A. Megrant, R. Barends, B. Campbell, B. Chiaro, A. Dunsworth, E. Jeffrey, J. Kelly, J. Mutus, P. J. J. O’Malley, C. Quintana, D. Sank, A. Vainsencher, J. Wenner, T. C. White, A. Polkovnikov, and J. M. Martinis. Ergodic dynamics and thermalization in an isolated quantum system. *Nature Physics*, 12:1037, 2016.
- [17] Shruti Dogra, Vaibhav Madhok, and Arul Lakshminarayan. Quantum signatures of chaos, thermalization, and tunneling in the exactly solvable few-body kicked top. *Phys. Rev. E*, 99:062217, Jun 2019.
- [18] Joanna K. Kalaga, Anna Kowalewska-Kudłaszyk, Mateusz Nowotarski, and Wiesław Leoński. Violation of leggett–garg inequalities in a kerr-type chaotic system. *Photonics*, 8(1), 2021.
- [19] A. W. van der Vaart. *Asymptotic Statistics*. Cambridge Series in Statistical and Probabilistic Mathematics. Cambridge University Press, 1998.
- [20] Joshua B. Ruebeck, Jie Lin, and Arjendu K. Pattanayak. Entanglement and its relationship to classical dynamics. *Phys. Rev. E*, 95:062222, 2017.
- [21] Sreeram PG, Vaibhav Madhok, and Arul Lakshminarayan. Out-of-time-ordered correlators and the loschmidt echo in the quantum kicked top: how low can we go? *Journal of Physics D: Applied Physics*, 54(27):274004, apr 2021.
- [22] Ryusuke Hamazaki, Kazuya Fujimoto, and Masahito Ueda. Operator noncommutativity and irreversibility in quantum chaos, 2018.
- [23] Rodolfo A. Jalabert, Ignacio García-Mata, and Diego A. Wisniacki. Semiclassical theory of out-of-time-order correlators for low-dimensional classically chaotic systems. *Phys. Rev. E*,

- 98:062218, Dec 2018.
- [24] Shenglong Xu and Brian Swingle. Scrambling dynamics and out-of-time-ordered correlators in quantum many-body systems. *PRX Quantum*, 5:010201, Jan 2024.
 - [25] T. Baumgratz, M. Cramer, and M. B. Plenio. Quantifying coherence. *Phys. Rev. Lett.*, 113:140401, Sep 2014.
 - [26] For a uniform random variable t_β , such a time average correctly gives the ensemble average for d_n . Same holds for higher moments.
 - [27] Roy J. Glauber and Fritz Haake. Superradiant pulses and directed angular momentum states. *Phys. Rev. A*, 13:357, Oct 1976.
 - [28] J M Radcliffe. Some properties of coherent spin states. *Journal of Physics A: General Physics*, 4(3):313–323, may 1971.
 - [29] Shohini Ghose, Rene Stock, Poul Jessen, Roshan Lal, and Andrew Silberfarb. Chaos, entanglement, and decoherence in the quantum kicked top. *Phys. Rev. A*, 78:042318, 2008.
 - [30] M V Berry. Evolution of semiclassical quantum states in phase space. *Journal of Physics A: Mathematical and General*, 12(5):625, may 1979.
 - [31] B.V. Chirikov, F.M. Izrailev, and D.L. Shepelyansky. Quantum chaos: Localization vs. ergodicity. *Physica D: Nonlinear Phenomena*, 33(1):77–88, 1988.
 - [32] Zbyszek P. Karkuszewski, Jakub Zakrzewski, and Wojciech H. Zurek. Breakdown of correspondence in chaotic systems: Ehrenfest versus localization times. *Phys. Rev. A*, 65:042113, Apr 2002.
 - [33] J. J. Sakurai and Jim Napolitano. *Modern Quantum Mechanics*. Cambridge University Press, 2 edition, 2017.